# Overlap interaction between spheroidal ions and the lattice dynamics of zinc and beryllium

D. B. Vibhute and M. P. Verma
*Department of Physics, Agra College, Agra-282002, India*
(Received 2 January 1975)

A phenomenological model of lattice dynamics of hcp metals has been developed by assuming the ions to have a spheroidal shape with the axis of revolution parallel to the $c$ axis. Overlap of spheroidal ions causes a noncentral interaction between the first neighbors (as in beryllium). The model is derived from a force system consisting of this noncentral overlap interaction, as six-neighbor central pair potential, and an electron-ion interaction term. Application of this model to zinc and beryllium shows that the force parameters coupling neighbors beyond the second are rather small as compared to the parameters for the first two neighbors. The dispersion curves derived from the model present a good agreement with the experimental curves.

## I. INTRODUCTION

Studies on lattice dynamics of hcp metals are usually based on well-known phenomenological models, viz., the tensor-force (TF),[1] the axially symmetric (AS),[2] and the modified axially symmetric (MAS)[3] models. These models consider the total interaction between ion pairs and do not give us any idea as to the constituent interactions that lead to the resultant force constants. Some of the recent models using ion-ion and ion-electron-ion interactions[4-6] should be considered in this sense somewhat better than the above models even though the ion-electron-ion interaction in these models is generally considered only in an approximate way. One of these recent models is that developed by Verma and Upadhyaya,[6] who derive the ion-ion interaction from a five-neighbor central pair potential. The potential parameters are usually determined through the equations for the five elastic constants and some of the lattice vibration frequencies at the zone center and zone boundaries. This model has explained the dispersion relations in many hcp solids in a satisfactory way. An application of this model to beryllium, however, leads to unsatisfactory results, and in the case of zinc the solution of the model equation leads to an imaginary value for a certain combination of force constants (usually called the optical correction). As against this, the MAS[3] describes the dispersion relations in beryllium and zinc to a satisfactory degree. It may be pointed out that the MAS arbitrarily distinguishes the bond-bending force constants in the basal plane from those perpendicular to the plane and thus makes the ion-ion interaction effectively noncentral.

The close packing of rigid spherical ions in the hcp structure gives an axial ratio $c/a = \sqrt{\frac{8}{3}} \simeq 1.63$. However, the measured values of $c/a$ vary over a significantly wide range around this ideal value. Phenomenologically this variation can be attributed to a spheroidal shape of the metal ions, the spheroids being surfaces of revolution around the $c$ axis. The close packing of prolate spheroids will give $c/a > \sqrt{\frac{8}{3}}$ (as in Zn) while the oblate spheroids will lead to $c/a < \sqrt{\frac{8}{3}}$ (as in Be). The axial ratio of the spheroids could be related to the observed $c/a$ ratio of the solid through a simple geometric analysis.

The overlap repulsion between ions must be directed along the line perpendicular to the common tangent plane at the point of contact. In the case of spheroidal atoms, this line goes through the centers of the overlapping ions only when the point of contact is along the principal axes. For contacts at the other points, the overlap of the two ions is necessarily noncentral. We have developed a new phenomenological model of lattice dynamics of hcp metals where we have added this noncentral interaction to the usual ion-ion and ion-electron-ion interactions.

The geometrical positions of neighbors of various orders are not the same in Be- and Zn-like solids. This, in general, leads to different mathematical expressions for the elements of the dynamical matrix in the two cases. However, if we collect contributions of all the neighbors up to certain orders (like the third, sixth, or eighth and so on), the two kinds of the hcp solids will give identical expressions for the dynamical matrix. This is why we have represented the central ion-ion interaction by a six-neighbor pair potential. The ion-electron-ion interaction has been derived from a modified Sharma-Joshi scheme. The new model differs from that of Verma and Upadhyaya essentially in having broken the first-neighbor interaction in two parts, viz., the overlap repulsion which is noncentral and the remaining central interaction which may be understood as the electrostatic ion-ion interaction. The application of this model to the relatively difficult

metals, beryllium and zinc, gives very satisfactory results.

## II. THE MODEL

Let us for convenience number neighbors as they would be in beryllium ($c/a<\sqrt{\frac{8}{3}}$). The position of the ion in the lattice is given by vectors $\vec{R}(l,\kappa)$, where $l=(l_1, l_2, l_3)$ is the cell index and $\kappa$ is the basis index. Let the origin ion be $(0,\kappa)$. The first neighbors of the origin ion will be of type $\kappa'\neq\kappa$. The axial ratio of spheroidal ions closely packing together to give the observed $c/a$ ratio can be easily proved to be

$$a_3/a_1=\sqrt{\tfrac{3}{8}}\,c/a\,, \tag{1}$$

where $a_1=a_2$ are the base semiaxes and $a_3$ is the semiaxis parallel to the $c$ axis. Denoting the Cartesian components of the position vector $\vec{R}(l,\kappa)$ as $X_\alpha(l,\kappa)$, we can derive the expression for the unit normal to the common tangent plane between the origin ion and the first neighbor at $\vec{R}(l',\kappa')$. Thus we find

$$\hat{\eta}(l',\kappa\kappa')=(X_1, X_2, \eta X_3)/(X_1^2+X_2^2+X_3^2)^{1/2}\,, \tag{2}$$

where,

$$\eta=\sqrt{\tfrac{8}{3}}\,a/c\,, \tag{3}$$

and, for simplicity, we have dropped the indices $(l',\kappa\kappa')$ on the right-hand side. The overlap of the ion will be determined by,

$$[\vec{u}(l',\kappa')-\vec{u}(0,\kappa)]\cdot\hat{\eta}(l',\kappa\kappa')=\vec{u}(l',\kappa\kappa')\cdot\hat{\eta}(l',\kappa\kappa')\,, \tag{4}$$

so that we can write the overlap potential in the form

$${}^R\phi(l',\kappa\kappa')=b'\exp\left(\frac{-\vec{u}(l',\kappa\kappa')\cdot\hat{\eta}(l',\kappa\kappa')}{\rho}\right). \tag{5}$$

This potential can be expressed in a more convenient form by introducing a factor $\exp\times[-\mathring{R}(l',\kappa\kappa')\cdot\hat{\eta}(l',\kappa\kappa')/\rho]$ with the relative equilibrium position $\mathring{R}(l',\kappa\kappa')$. Thus we have

$${}^R\phi(l',\kappa\kappa')=b\exp\left(\frac{-\vec{R}(l',\kappa\kappa')\cdot\hat{\eta}(l',\kappa\kappa')}{\rho}\right). \tag{6}$$

Differentiating this potential twice with respect to the coordinates, we obtain the force constants

$$\left(\frac{\partial^2{}^R\phi(l',\kappa\kappa')}{\partial X_\alpha(l',\kappa\kappa')\partial X_\beta(l',\kappa\kappa')}\right)_0=\left(\frac{{}^R\phi}{\rho^2}\,\frac{\partial\vec{R}(l',\kappa\kappa')\cdot\hat{\eta}(l',\kappa\kappa')}{\partial X_\alpha(l',\kappa\kappa')}\times\frac{\partial\vec{R}(l',\kappa\kappa')\cdot\hat{\eta}(l',\kappa\kappa')}{\partial X_\beta(l',\kappa\kappa')}-\frac{{}^R\phi}{\rho}\,\frac{\partial^2\vec{R}(l',\kappa\kappa')\cdot\hat{\eta}(l',\kappa\kappa')}{\partial X_\alpha(l',\kappa\kappa')\partial X_\beta(l',\kappa\kappa')}\right)_0. \tag{7}$$

The derivatives involved in this equation yield cumbersome expressions. We can, however, retain the important terms leaving remainders which are necessarily small and thus express the force constants as

$$\left(\frac{\partial^2{}^R\phi(l',\kappa\kappa')}{\partial X_\alpha(l',\kappa\kappa')\partial X_\beta(l',\kappa\kappa')}\right)_0=\lambda\,\frac{x_\alpha x_\beta}{r^2}-\mu\,\frac{1}{r}\left(\delta\alpha\beta-\frac{x_\alpha x_\beta}{r^2}\right), \tag{8}$$

where we have put

$$\vec{r}=(x_1, x_2, x_3)=(X_1X_2\eta X_3), \tag{9}$$

$${}^R\phi/\rho^2=\lambda\,,\quad\text{and}\quad {}^R\phi/\rho=\mu\,. \tag{10}$$

These force constants are now used to compute the coupling coefficients

$$\mathfrak{D}^R_{\alpha\beta}(\vec{q},\kappa\kappa')=-\sum\left(\frac{\partial^2{}^R\phi(l',\kappa\kappa')}{\partial X_\alpha(l',\kappa\kappa')\partial X_\beta(l',\kappa\kappa')}\right)\times\exp[-i\vec{q}\cdot\vec{R}(l',\kappa\kappa')], \tag{11}$$

where the summation is to be made over only such $l'$ indices which refer to the six first neighbors of the origin atom at $(0,\kappa)$.

The coupling coefficients so obtained are added to those derived from the six-neighbor central pair potential to give the complete ion-ion coupling coefficients.

The electron ion coupling coefficients used by Verma and Upadhyaya are

$$\mathfrak{D}^e_{\alpha\beta}(\vec{q},\kappa\kappa')=\begin{cases}K_e\,q_\alpha q_\beta G^2\Omega\,, & \kappa=\kappa'\\ 0\,, & \kappa\neq\kappa'\,,\end{cases} \tag{12}$$

where $K_e$ is the bulk modulus of the electron gas, $q_\alpha$ is the phonon wave vector, $\Omega$ is the unit cell volume, and

$$G=3(\sin\lambda' q-\lambda' q\cos\lambda' q)/(a_1^2q_1^2+a_2^2q_2^2+a_3^2q_3^2)^{1/2}\,,$$

where $\lambda'$ is given by $\lambda'=(a_1^2q_1^2+a_2^2q_2^2+a_3^2q_3^2)^{1/2}/q$, $q=|\vec{q}|$;

$q_1$, $q_2$, and $q_3$ are the components of $\vec{q}$ along the three semiaxes $a_1$, $a_2$, and $a_3$ of the atomic spher-

oid.

The assumption that $\mathfrak{D}^e_{\alpha\beta}(\vec{q}, \kappa\kappa') = 0$ for $\kappa \neq \kappa'$ is arbitrary, and is, in fact, incompatible with the hcp structure having two atoms per unit cell. The Sharma-Joshi theory determines the strain energy of the electron gas due to a plane wave propagating through the gas. The motion of the wave front containing the ion is identical with the motion of the ion. The ion-electron coupling coefficient expressed in Eq. (12) has been determined by averaging the strain energy of the electron gas over the atomic polyhedron around the ion at the center. Now let us consider the motion of the electron gas at the boundary between the two polyhedra of the two neighboring ions $\kappa \neq \kappa'$. Since the two ions vibrate independently of each other in a lattice mode, the boundary layer of the electron gas seems to have two very different displacements at the same time. This is certainly not correct. We can overcome this difficulty by averaging the strain energy over a unit cell which is the periodic repeat unit of the crystal by assigning an element of the electron gas a displacement which is the resultant of the two independent plane waves starting from the two ions. The procedure leads to a nonzero coupling between the two ions. Summed over the six first neighbors, this coupling results in the coefficients

$$\mathfrak{D}^e_{\alpha\beta}(\vec{q}, \kappa\kappa') = \frac{K_e}{6} \sum_{\text{first neighbors}} q_\alpha q_\beta G^2 \Omega \times \exp[-i\vec{q}\cdot\vec{R}(l'\kappa\kappa')], \quad \kappa \neq \kappa', \qquad (13)$$

with

$$\mathfrak{D}^e_{\alpha\beta}(\vec{q}, \kappa\kappa) = K_e q_\alpha q_\beta G^2 \Omega .$$

The parameter $K_e$ in Eq. (13) differs from that in Eq. (12) by a factor $\frac{1}{4}$, but since $K_e$ is an undetermined parameter in the theory, this difference is immaterial.

TABLE I. Input data for Zn. $a = 2.660$ Å, $c = 4.88$ Å, $m = 65.37$ amu, $c/a = 1.8346$.

| | |
|---|---|
| Elastic constants ($10^{12}$ dyn cm$^{-2}$) | $C_{11} = 1.791$, $C_{12} = 0.375$, $C_{33} = 0.688$, $C_{44} = 0.4595$, $C_{13} = 0.554$ |
| Phonon frequencies (THz) | $\nu_{LO}(\Gamma) = 4.57$, $\nu_{TO}(\Gamma) = 2.29$, $\nu_{LA}(A) = 2.92$, $\nu_{TA\perp}(M) = 2.02$, $\nu_{TO\perp}(M) = 2.70$, $\nu_{TA\parallel}(M) = 3.52$, $\nu_{TO\parallel}(M) = 3.72$, $\nu_{LA}(M) = 6.11$, $\nu_{LO}(M) = 6.44$ |

TABLE II. Input data for Be. $a = 2.2856$ Å, $c = 3.5832$ Å, $m = 9.012$ amu, $c/a = 1.5677$.

| | |
|---|---|
| Elastic constants ($10^{12}$ dyn cm$^{-2}$) | $C_{11} = 2.923$, $C_{12} = 0.267$, $C_{33} = 3.364$, $C_{44} = 1.625$, $C_{13} = 0.140$ |
| Phonon frequencies (THz) | $\nu_{LO}(\Gamma) = 20.1$, $\nu_{TO}(\Gamma) = 13.75$, $\nu_{LA}(A) = 15.00$, $\nu_{TA\perp}(M) = 12.60$, $\nu_{TO\perp}(M) = 17.00$, $\nu_{TA\parallel}(M) = 11.75$, $\nu_{TO\parallel}(M) = 16.60$, $\nu_{LA}(M) = 16.00$, $\nu_{LO}(M) = 16.82$ |

## III. CALCULATIONS AND RESULT

The total number of parameters described in Sec. II are 15, viz., the 12 central potential parameters $\alpha_i$, $\beta_i$ $(i = 1, \cdots, 6)$, the two overlap parameters $\lambda$, $\mu$, and the bulk modulus of the electron gas, $K_e$. These parameters were determined from the five elastic constants $C_{ij}$, the rotational-invariance condition, and nine chosen frequencies $\nu$ at the zone center and zone boundaries. It was found that the parameters $\alpha_2$, $\alpha_5$, and $\alpha_6$ could not be determined from the equations used, as the latter invariably lead to the same combinations of these parameters. In the ordering of the neighbors used by us, the sixth neighbor in beryllium is the farthest among second, fifth, and sixth, while in zinc it is the fifth neighbor which is the farthest of the three. Hence the solution for these parameters $\alpha_2$, $\alpha_5$, and $\alpha_6$ was obtained by arbitrarily assigning various values to $\alpha_6$ in beryllium and $\alpha_5$ in zinc and then choosing those values which gave us the best agreements with the dispersion curves. The input data used are given in Tables I and II, and the values of the parameters finally used in the calculations are listed in Tables III and IV. These values show that the strongest contributions to the force system came from the first two neighbors, the coupling due to the relatively distant neighbors being rather weak as it reasonably should be. The model leads to the dispersion curves for the [0001] and [01$\bar{1}$0] directions, as shown in Figs. 1 and 2.

TABLE III. Evaluated force parameters for Zn in units of $10^4$ dyn cm$^{-1}$ and bulk modulus of the electron gas ($K_e$) in $10^{12}$ dyn cm$^{-2}$.

| |
|---|
| $\alpha_1 = -9.103$, $\alpha_2 = -0.370$, $\alpha_3 = +0.003$, $\alpha_4 = +0.148$, $\alpha_5 = +0.173$, $\alpha_6 = +0.116$, $\beta_1 = +0.822$, $\beta_2 = +2.903$, $\beta_3 = +0.154$, $\beta_4 = -0.455$, $\beta_5 = -0.289$, $\beta_6 = +0.120$, $\mu = +8.967$, $\lambda = +7.803$, $K_e = +0.143$ |

TABLE IV. Evaluated force parameters for Be in units of $10^4$ dyn cm$^{-1}$ and bulk modulus of the electron gas ($K_e$) in $10^{12}$ dyn cm$^{-2}$.

$\alpha_1 = +0.261$, $\alpha_2 = +8.802$, $\alpha_3 = -0.049$, $\alpha_4 = +0.327$, $\alpha_5 = +0.300$, $\alpha_6 = -0.100$, $\beta_1 = +1.301$, $\beta_2 = +3.467$, $\beta_3 = +0.141$, $\beta_4 = -0.364$, $\beta_5 = -0.469$, $\beta_6 = +0.456$, $\mu = -8.684$, $\lambda = -15.488$, $K_e = +0.529$

The curves for beryllium present a good fit to the experimental curves of Roy *et al.*[7] except for the $\Sigma_1^u$ branch in the [01$\bar{1}$0] direction. Similarly, in the case of zinc the agreement with the experimental points of Almqvist *et al.*[8] is excellent, except in the case of the $\Sigma_3^L$ branch in the [01$\bar{1}$0] direction. However, our curves for both Be and Zn are at least as good as those of de Wames *et al.*,[3] who essentially use a 19-parameter model as against our 15-parameter one. It is true that the model of de Wames *et al.* uses a smaller number of parameters in the case of beryllium, but that has been possible by using an artificial constraint among the bond-bending force constants. Our curves in the case of Zn are almost identical with those of de Wames *et al.* In the case of Be, however, the MAS calculations lead to a much better $\Sigma_1^u$ branch, but the $\Sigma_2^u$ branch goes very much off the experimental curve. We could reproduce the MAS curves by varying $\alpha_6$, but the curves obtained by us (shown in Fig. 2) perhaps present a better overall agreement with experiment than the MAS curves of de Wames *et al.* If we assume the three principal axes of the spheroid to be equal, our model will reduce to the central-pair-potential

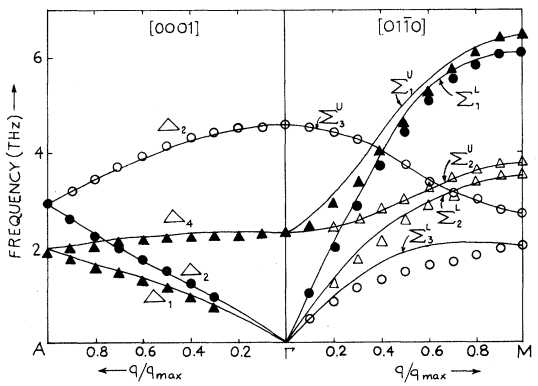


FIG. 1. Dispersion curves of Zn in the principal symmetry directions. Triangles and circles show the experimental points (Ref. 7). Solid lines show results from our theoretical calculations.

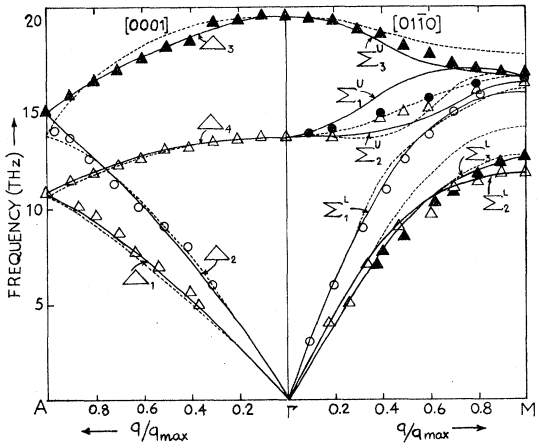


FIG. 2. Dispersion curves of Be in the principal symmetry directions. Triangles and circles show experimental points (Ref. 10). Solid lines show results from our theoretical calculations. The dashed lines show Verma and Upadhyaya's results (Ref. 6).

model of Verma and Upadhyaya[6] (see also Upadhyaya and Verma[9,10]). In the case of zinc, their model leads to imaginary values for some of the parameters, and for beryllium their curves, shown by dashed lines in Fig. 2, show much larger deviations. Thus the assumption of spheroidal ions not only explains the deviation of the $c/a$ ratio from the ideal value $\sqrt{\frac{8}{3}}$, but it also gives a sufficiently good description of the dispersion relations and, in fact, reproduces the MAS results exactly. It is evident that the artificial assumption of the MAS can be replaced by a more plausible assumption of spheroidal ions constituting the hcp system.

A recent work on the lattice dynamics of beryllium by Roy *et al.*[7] shows that certain degeneracy properties of frequencies at the zone boundary in the [11$\bar{2}$0] direction cannot be satisfied by a central potential or axially symmetric forces, while a second-neighbor tensor force leads to the observed degeneracy. We have, therefore, checked to see if the overlap interaction used in the present work gives the desired results. Unfortunately it does not. Bertoni *et al.*[11] have presented first-principles calculations of the dispersion curves of beryllium which include the third-order terms in the electron-ion pseudopotential. This scheme is equivalent to including a three-body interaction in the force system and leads to the correct explanation of the dispersion relations. Therefore, the inclusion of a three-body interaction in our model may remove the small errors appearing in our calculations and lead to a better explanation of the disperion relations in hcp solids in general.

[1]M. Born and G. H. Begbie, Proc. R. Soc. A 188, 179 (1947).
[2]G. W. Lehman, T. Wolfram, and R. E. De Wames, Phys. Rev. 128, 1593 (1962).
[3]R. E. De Wames, T. Wolfram, and G. W. Lehman, Phys. Rev. 138, A717 (1965).
[4]S. S. Kushwaha and J. S. Rajput, J. Phys. F 1, 377 (1971).
[5]M. M. Shukla and J. B. Salzberg, Phys. Lett. A 43, 429 (1973).
[6]M. P. Verma and J. C. Upadhyaya, Solid State Commun. 13, 779 (1973).
[7]A. P. Roy, B. A. Dasnnacharya, C. L. Thapar, and P. K. Iyengar, Phys. Rev. Lett. 30, 906 (1973); 30, 1278E (1973).
[8]L. Almqvist and R. Stedman, J. Phys. F 1, 785 (1971).
[9]J. C. Upadhyaya and M. P. Verma, Phys. Rev. B 8, 593 (1973).
[10]J. C. Upadhyaya and M. P. Verma, J. Phys. F 3, 640 (1973).
[11]C. M. Bertoni, V. Bortolani, C. Calandra, and F. Nizzoli, Phys. Rev. Lett. 31, 1466 (1973).